Renewable Energy 101 (2017) 1141–1156

Contents lists available at ScienceDirect

Renewable Energy

journal homepage: www.elsevier.com/locate/renene

Computational prediction of pressure change in the vicinity of tidal stream turbines and the consequences for fish survival rate

E. Zangiabadi [a], I. Masters [a], Alison J. Williams [a], T.N. Croft [a], R. Malki [a], M. Edmunds [a, *], A. Mason-Jones [b], I. Horsfall [c]

[a] College of Engineering, Swansea University, SA1 8EN, UK
[b] School of Engineering, Cardiff University, CF24 3AA, UK
[c] College of Science, Swansea University, SA2 8PP, UK

ARTICLE INFO

Article history:
Received 25 September 2015
Received in revised form
22 September 2016
Accepted 25 September 2016

Keywords:
Marine energy
Tidal stream turbine
CFD
Fish
Marine environment

ABSTRACT

The presence of Tidal Stream Turbines (TST) for tidal power production, leads to changes in the local physical environment that could affect fish. While other work has considered the implications with respect to conventional hydroelectric devices (i.e. hydroelectric dams), including studies such as physical impact with the rotors and pressure variation effects, this research considers the effects of sudden changes in pressure and turbulence on the hypothetical fish with respect to TSTs. Computational fluid dynamics (CFD) is used to investigate changes to the environment, and thus study the implications for fish. Two CFD methods are employed, an embedded Blade Element representation of the rotor in a RANS CFD model, and a blade resolved geometry using a moving reference frame. A new data interpretation approach is proposed as the primary source of environmental impact data; 'rate of change of pressure' with time along a streamtrace. This work also presents results for pressure, pressure gradients, shear rates and turbulence to draw conclusions about changes to the local physical environment. The assessment of the local impact is discussed in terms of the implications to individual fish passing a single or array of TST devices.

1. Introduction

Marine renewable energy is becoming a viable source of energy production as the sector develops and grows. Across the world technologies are being engineered to address the issues of energy extraction in these environments. However, research into the environmental impact of marine devices remains incomplete. This is due, in part, because many of the devices have yet to be deployed and tested [1,2]. As the sector moves towards grid connected prototype devices, the industry attention is turning toward assessing the environmental impact of deployment. Of the key types of marine energy extraction approaches it is tidal stream devices (i.e. tidal stream turbines) that this work seeks to inform.

Tidal Stream Turbines (TST's, also known as Marine Hydro Kinetic (MHK) turbines) are rotating lift devices which are capable of extracting kinetic energy from a moving body of water, converting it into more useful electrical energy [3]. To best utilise this approach TST's are placed in locations of predictable high tidal flow rates. The interaction of these lift devices (rotating hydrofoils) with the local fluid flow generates pressure gradients and turbulence which otherwise would not be seen in the region [4]. The effect of these devices on the local environment is studied in this paper paying attention to how this change in habitat may effect the local fish population. The locations suitable for the installation of TST's are usually estuaries and channels [5] which are home to various fish species. When considering a potential TST installation site, key issues such as the interaction of these devices with the local environment must be examined.

Among the most obvious risks that fish encounter when interacting with TST's is the risk of being hit by the turbine hydrofoils. There have been a number of studies which investigated the chance of a species being hit by the rotating hydrofoils. A previous study shows that for different scenarios, a collision chance of 6%–19% exists for fish with an expected chance of survival of more than 96% [6]. Another study on the possibility of hydrofoil strike indicates that this issue depends on the fish size, turbine dimensions, and the specification of the deployment site. However, the risk of hydrofoil

* Corresponding author.
E-mail address: m.edmunds@swansea.ac.uk (M. Edmunds).

http://dx.doi.org/10.1016/j.renene.2016.09.063

strike is higher for larger fish [7]. Another behaviour study shows that although fish were always present in the wake of a TST, the probability of them entering the hydrofoil region is 35% lower when it is rotating and then fish have a tendency to avoid the hydrofoil in the same way that they avoid other objects such as trawls. Schools of fish have about 56% lower probability to enter the turbine in comparison with the individuals [8,9].

Apart from the hydrofoil strike risk, another major threat for the fish is the rapid pressure change in the turbines swept area. There is a pressure increase in front of the turbine which is followed by a sudden pressure drop immediately behind the turbine. Then the pressure gradually increases again to the ambient/freestream pressure [10]. A potential cause of mortality during passage through a conventional hydroelectric turbine (i.e. a hydroelectric dam), is damage to internal organs as a result of significant pressure change [11] [12]. also studied the passage of fish through a conventional hydroelectric turbine, and established that other common reasons for injury are cavitation and turbulence.

For conventional hydroelectric turbines, cavitation happens at a very small area near the trailing edge of the hydrofoil [13]. This region is small when compared to the size of the turbine and the fish. TSTs are designed to operate only at optimal efficiency, and thus the occurrence of cavitation is minimal. With this is mind, cavitation-related injuries are likely very small if not negligible [14]. Further to this, the computational study and findings by Ref. [15] have shown that cavitation effects are negligible, and thus will not be discussed in detail in this paper.

Research by Ref. [16] shows that damage to internal organs and disorientation happen during the rapid passage through a conventional hydroelectric turbine. A study conducted on the migration of fish in the Bay of Fundy revealed that, depending on the species, the mortality rate is between 20 and 80% per passage. However, the turbine used in this study is similar to conventional hydroelectric turbines (i.e. a closed in turbine at a tidal barrage facility) and, because of the design of this device, mechanical strike is the main cause of mortality [17].

In this paper a computational fluid dynamics (CFD) virtual experiment is used to investigate changes to the local environment when installing TST's. This work examines the case of a single TST operating in a 6 knot flow, and the case of a three rotor array of TST's with emphasis on the near rotor domain. This data is then used to assess the survival of rate of the fish population passing through a TST (or multiple TST's) by measuring the time that the fish are exposed to significant pressure/velocity variations. The Blade Element Momentum CFD (BEM-CFD) approach [18] and a full CFD simulation with complete hydrofoil geometry, which here is referred to as blade resolved geometry (BRG) [19], is used to predict the effect of the TST's interaction with the local environment.

By determining the pressure differences fish are exposed to, it is also possible to determine the potential risk of harm to the fish. An example is the volume change of the fish swim bladder (where applicable) when passing through a region of significant pressure variation. Experiments show that the swim bladders' volume change is related to Boyles law [20]. This can then be used to estimate the survival rate of the fish (with regards the swim bladder), provided that there are experimental observations for the species concerned.

This research makes two simplifying assumptions; firstly that the fish does not exhibit any avoidance behaviour and swim in the natural direction of the flow, and secondly that there is no physical contact of the hydrofoil with the fish. Although fish may attempt avoidance in such scenarios [7,8], this study simplifies this behaviour based on the premise that avoidance is a function of device size (larger devices have lower rotational speed), flow speed and fish size, i.e. relatively smaller fish moving in a fast current passing through a large slow moving device, as would be the case with a device maximised for power extraction placed in an ideal tidal stream site. Obviously, any avoidance behaviour will improve outcomes for fish survival.

2. Literature review

The literature presented in this section details the different phenomena that could cause injury to fish during the passage through a conventional hydroelectric turbine [14]. A conventional hydroelectric turbine is referred to in this work in the context of a closed housing surrounding the turbine set in some larger structure, i.e. a hydroelectric dam, barrage or lagoon. While the literature to date has focussed on conventional hydroelectric turbines [14], this work seeks to extend the research topic to cover interactions with open hydrofoil TSTs. This section starts by highlighting the key interactions of conventional hydroelectric turbines, and then seeks to highlight the important differences with TSTs.

Environmental effects of conventional hydroelectric turbines:

- Rapid and excessive pressure changes.
- High shear and turbulence levels.
- Cavitation.
- Grinding and abrasion between moving and stationary components.
- Leading edge hydrofoil strike.

The key operational differences between conventional hydroelectric turbines and TST designs are [14,22]:

- Conventional hydroelectric turbines are situated in a housing designed to channel fluid into the turbine. In contrast TSTs operate in an open environment.
- In a conventional hydroelectric turbine the head difference contributes to a large pressure change across the turbine. In contrast, a TST has no significant head difference, and thus a relatively small pressure change.
- TSTs operate at lower angular velocities (rotational speed) compared to conventional hydroelectric turbines.

In the remainder of this section, literature (within the scope of this study) reviewing the environmental effects potentially leading to fish injury is examined. The literature is subdivided into; Rapid and Excessive Pressure Change (Subsection 2.1), and High Shear and Turbulence (Subsection 2.2).

2.1. Rapid and excessive pressure change

In hydroelectric dams the low head axial flow Kaplan turbine is a commonly used design. As a fish passes through a Kaplan turbine the most extreme conditions happen near the intake ceiling and the tip of the blade. Along this journey the pressure is increased by nearly 140 kPa and can reach up to 340 kPa. Immediately after the blade disk, the pressure drops to nearly 2 kPa. The lowest pressure that the fish experiences is called the Nadir and the total time that the fish is exposed to this pressure is nearly 0.25 s. Immediately after this drop to the nadir, the pressure rapidly increases to reach the atmospheric pressure in the draft tube and tailwaters [23]. These rapid pressure fluctuations can cause injury and mortality for the fish [11] due to volume changes in the swim bladder in proportion to Boyles Law [24].

The research that has been done to investigate the effects of pressure changes on fish is very species specific and mostly carried out for a certain location and a particular turbine design. Previous research includes the survival rate of *Lepomis macrochirus* (Bluegill

Sunfish), Juvenile *Oncorhynchus tshawytscha* (Fall Chinook Salmon), *Oncorhynchus mykiss* (Rainbow Trout), *Gadus morhua* (cod), and *Pollachius Viren* saithe/coley, etc. [11,25,26].

[11] conducted an experiment during which the water pressure increased either from 101 kPa or 191 kPa to nearly 400 kPa over 30–60 s to simulate the fish entry to the intake and runner channel of a conventional hydroelectric turbine. Fish then encountered a sudden (0.1 s) pressure drop to 2–10 kPa (Chinook salmon, rainbow trout, and bluegill) or about 50 kPa (Chinook salmon and bluegill) followed by a very rapid increase (again in 0.1 s) to 191 kPa before returning to atmospheric pressure.

Sixteen to twenty four hours before the start of the experiment, the species were pressure acclimated for surface pressure (101 kPa) and 30 ft (192 kPa) depth. Fig. 1 tracks simulated fish passage through a Kaplan turbine. The type of injuries observed in the experiment by [11] included; black spots on the top of the head, gradually developed overinflation of the swim bladder, internal haemorrhaging of blood vessels near the swim bladder, ruptured swim bladders, massive gas bubbles in the heart and gas bubbles in the afferent lamellar arteries of the gills. While the last three injuries all caused death, the most common cause of mortality was a ruptured swim bladder. The resulting injury mortality rate predictions for Bluegill Sunfish, Fall Chinook Salmon and Rainbow Trout are summarised in Table 1.

These types of experiments are usually carried out using closed pressurised chambers in which the water pressure is precisely controlled primarily using mechanical means or sometimes underwater explosions [27]. Regardless of the method used, the species has to be acclimatised to a certain pressure (usually near surface pressure i.e. atmospheric) before being exposed to the sudden pressure variation. The results of several experiments showed that pressure gradients above 90 kPa/s can cause substantial damage to fish and increase mortality rates [28].

The other pressure related issue for the species is the pressure change in the wake of a conventional hydroelectric turbine. After passing the turbine and entering its wake the fish will experience

Table 1
Nadirs[a] at which mortality/injury appears to be negligible during a one-time exposure (first three columns from Ref. [11]). Pressure drop here is the quantity of pressure change as the fish swim their course.

Species	Death	Injury	Pressure drop
Bluegill Sunfish	~50 kPa[b]	>50 kPa	350 kPa
Fall Chinook Salmon	2–10 kPa	2–10 kPa	390 kPa 398 kPa
Rainbow Trout	2–10 kPa	2–10 kPa	390 kPa 398 kPa

[a] Lowest pressure in kiloPascals (kPa).
[b] Since the Bluegill injury rate at approximately 50 kPa appeared to be substantial and the injury rate at 68 kPa and 95 kPa could not be evaluated, a higher, currently unknown, nadir is suggested.

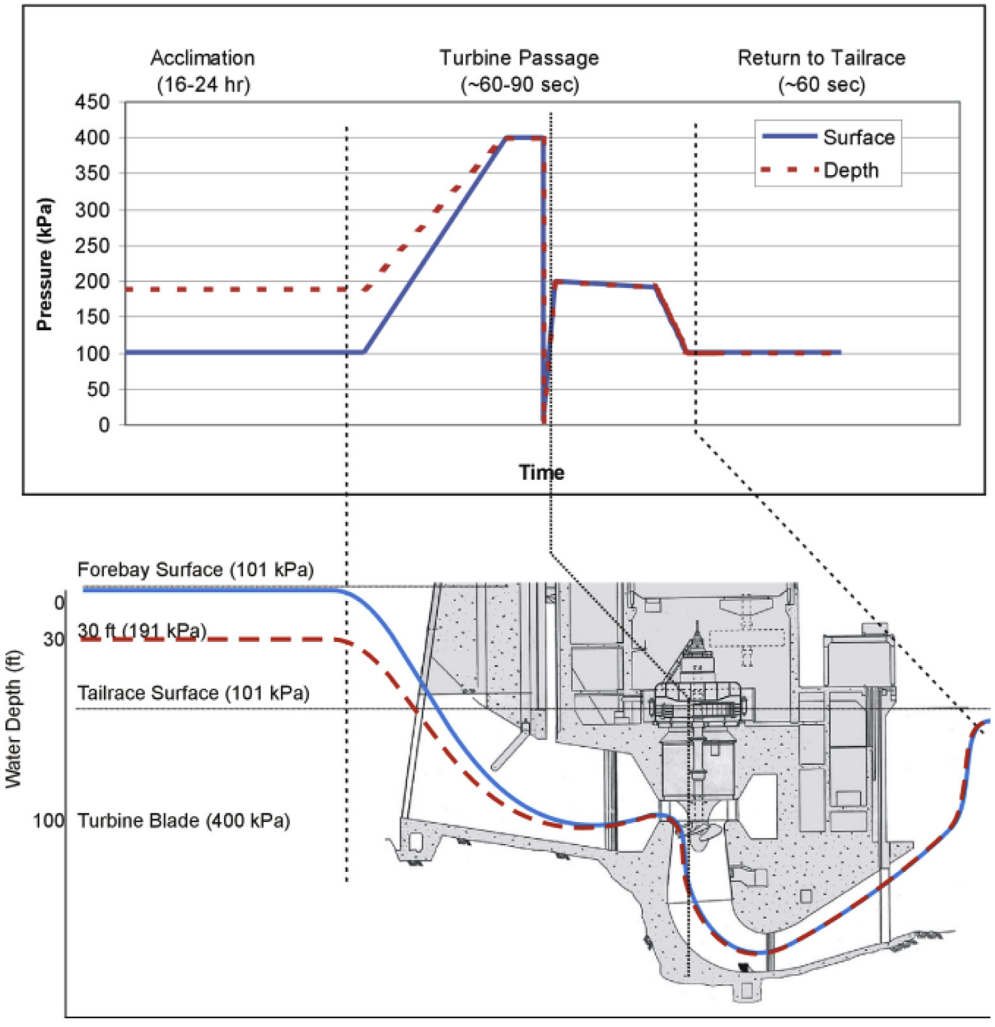

Fig. 1. Pressure exposure simulation of turbine passage for surface and depth acclimated Fish for Kaplan Turbine; source [11].

wake swirl and turbulent eddies. The fish will move vertically in the water column (both upward and downward) while swimming away from the hydrofoils. Under normal circumstances travelling in the water column occurs gradually to allow time for the swim bladder to expand or contract. However, in the turbulent region behind a conventional hydroelectric turbine, the rapid pressure fluctuations can also affect fish survival rates.

This paper aims to show that the pressure differential across a TST is significantly smaller than that found in a conventional hydroelectric turbine, and thus the resultant effect on the local fish population is likely diminished. The wake from a TST however is still characterised by wake swirl and turbulent eddies, although to a lesser extent as the rotational speed of the TST is less than that of a conventional hydroelectric turbine.

2.2. High shear and turbulence

During passage through a conventional hydroelectric turbine, fluid will be subject to both shear and turbulence. The high shear and accelerative forces are attributed to the changes in bulk flow speeds, while the turbulence is attributed to small-scale velocity variations when interacting with turbine geometry [26]. When fish are exposed to these phenomena, it is recognised as a potential danger to the species [29]. The forces can cause rotation and deformation of the fishes' body surface and thus potentially lead to injury or mortality [14].

In conventional hydroelectric turbines, the turbulence is determined by two factors. The first one is the turbulence length scale which describes the size of eddies in the turbulent flow, and the second one is the turbulence intensity. Small and large scale turbulence occurs at different locations in a conventional hydroelectric turbine. The large scale turbulence usually occurs within the turbine draft tube [29], while the small scale turbulence tends to occur in the turbine passageways and in the wake of the runner blades [30]. The effects of the small and large scale turbulence on fish are different. The small scale turbulence can twist and compress portions of the fishes' body while the large scale turbulence can generate vortices which spin the fish and may cause disorientation. The large scale turbulence may not directly damage the fish but the disorientation of fish which have passed through the turbine may make them prone to be hunted by predators [29].

When evaluating environmental risk to the fish [26], noted that a useful measure is the shear stress at the fishes' body surface. Table 2 shows values for shear stress that have been reported for various natural and man-altered aquatic environments. The estimated values of shear stress in streams and rivers under normal flows are generally low (less than 100 N/m^2). These locations are the natural habitat of the species so it can be assumed that these values are not harmful [21].

In contrast, a report by Ref. [31] showed that velocity within a conventional hydroelectric turbine can vary from zero near to the solid boundaries up to 6 m/s away from the boundary layer, where the shear rate can be as high as 30/s. The fish are exposed to a greater magnitude of shear stress in this environment relative to what they experience in their natural habitat [14].

Most of the data for shear stress affected fish comes from laboratory experiments. In these studies the fish are exposed to a high speed water jet in a static water tank. The disadvantage of these experiments is that the shear values are only applied to a portion of the fish. Some of the results of such experiments are [26]:

- 3410 N/m^2 (34,100 $dynes/cm^2$; 3.4 kPa) caused no apparent injury and no mortality among eels.
- 1920 N/m^2 (19,200 $dynes/cm^2$; 1.9 kPa) caused low levels (~10%) of injury and mortality to juvenile salmonids.
- 206 N/m^2 (2060 $dynes/cm^2$; 0.2 kPa) can cause complete mortality in clupeids (herring), apparently due to loss of scales, epithelium, and mucous layers.
- 35 N/m^2 (350 $dynes/cm^2$; 0.035 kPa) caused an average of 38% mortality among white perch larvae exposed for 1 min, 52% for 2 min, and 75% for 4 min. Striped bass larvae were nearly as sensitive.

The total amount of shear to which the fish are exposed was not fully quantified by the jet nozzle experiments. To overcome this issue, later studies have used computer models to predict shear forces in the different phases of a conventional hydroelectric turbine near the blades and other structures [14] [30]. used CFD techniques to investigate the risk of shear related injuries in small low-head (<10 m) Francis and Kaplan turbines, and showed that fish injury caused by shear stress is a less important issue in both types of turbines because of the low probabilities of occurrence.

A comprehensive study to assess the biological response of different species to various levels of shear stress was reported in Ref. [21]. Shear stress values were first predicted using CFD methods, and then the same situations were replicated using a large flume and a water jet nozzle. The results showed that the effects of shear stress on the individual fish was related to the relative velocity and orientation of the fish to the flow, and to the shape of the fish. Another experiment by Ref. [32] studied juvenile salmonids, assessing the injury and mortality rates when exposed to a shear zone. The injury severity was higher in a case where the fish entered head first into the shear zone in comparison to tail first entry [32]. In Ref. [33] CFD methods were employed to identify the maximum values of strain rates and the location in which the values are extreme.

Recent multi-disciplinary research [12] revealed that the highest value of shear stress occurs in or near the stay vanes and wicket gates, runner, and draft tube of a conventional hydroelectric turbine. These features do not exist in most TST designs. Therefore, although the physical effects of shear and turbulence are similar, it is very unlikely that the magnitude of strain rates generated in TSTs will be significant to fish mortality rates. Although there is stress and disorientation for a fish as it goes through the turbine, the

Table 2
Published estimates of shear stress (N/m^2) in natural and man-altered aquatic environments (Table 5.1 in Ref. [21]).

Environment	Shear stress (N/m^2)	Literature cited
Water column in a trout stream, average flow	<1.0	Fausch and White (1981)
Small streams, near bed	<1–7	Lancaster and Hildrew (1993)
Medium-size streams, near bed (90 measurements)	most <30, some >200	Statzner and Mller (1989)
Flash floods, small basins	61–2600	Costa (1987)
Floods, large rivers	6–10	Costa (1987)
Bulb turbine draft tube	500–5421	McEwen and Scobie (1992)
Near ship hulls and wakes	7.6–40.4	Morgan et al. (1976)
Near barge propeller	>5000	Killgore et al. (1987)

hydraulic conditions associated with TSTs are expected to be more 'fish-friendly' [14] and investigation of this hypothesis is one of the aims of this paper.

3. Numerical methods

Two different approaches are used to simulate flow around a tidal stream turbine. The first approach is the Blade Element Momentum (BEM-CFD) method where the turbine effects are time averaged to a swept area so that the influence of the hydrofoils (chord, twist, etc.) varies according to radial position [18], but neglects circumferential variations. The second method takes into account the full turbine Blade Resolved Geometry (BRG) [34]. The remainder of this section discusses the methodology of modelling TSTs including details of the three cases used in this study.

3.1. Model methodology

The single device model has a 10 m diameter turbine in a rectangular domain with the dimensions of 506 m × 50 m × 50 m. The turbine is located 104 m from the inlet to allow the flow to settle before reaching the turbine. For the BRG model, the turbine geometry consists of 3 blades and a nacelle where the centre of the rotor is positioned centrally in respect to the height and width of the channel (Fig. 2). The meshed domain consists of approximately 1.18 million tetrahedral elements. Uniform flow with a speed of 3.086 m/s (6 knots) is set for the inlet and the bed is defined to be a non-slip wall. Values of inlet turbulence of 0% (CFD-BEM) and 5% (BRG) were applied to the model, however this dissipates significantly due to the numerical scheme chosen and has minimal effect on the flow compared to the presence of the rotor. The blade surfaces have a wall boundary condition imposed whereas for all the side walls and the top of the domain symmetry boundary conditions have been enforced. The outlet of the domain is set to have an outflow boundary condition in which Fluent® considers a zero diffusion flux for all flow variables. To run the simulation, the rotational speed of the blade is set to 2.25 rad/s (optimum rotational speed), where the rotational zone has 17 m diameter and 6 m width [19,34].

For the CFD-BEM method, again a 10 m diameter rotor is considered and a mesh consisting of 6.03 million tetrahedral elements has been used. A cuboid box of higher mesh density is placed around the blade region (Fig. 3). The physical properties of the turbine are represented as a source term where the chord and twist values of the blade match those used in the BRG model. All the boundary conditions are defined in the same way as the BRG model.

In reality, TSTs will be in an array and the fish which goes through a TST could pass through an array of TSTs. In order to investigate this, a triangular configuration of TSTs was set up. Only the BEM-CFD method was used to study the tidal array scenario.

Fig. 4 shows the model set up resembling a channel with 700 m length, 200 m width and the water depth of 30 m in which the vertical coordinate of the turbines centre is located half way through the depth. The first row of the turbines is located 300 m from the inlet. The configuration has two turbines in the first row which are 15 m apart and the second row turbine is located 75 m downstream at a lateral position that is midway between the first row of turbines to form a triangular shape TST array. This layout is a simple geometry that allows simulation of the case in which the species goes through two rows of turbines.

To have a direct comparison between the two models, a standard finite volume approach with a $k-\varepsilon$ turbulence model has been employed to conduct both simulations. Pressure-velocity coupling uses the SIMPLE algorithm and for spatial discretisation of the momentum, turbulent kinetic energy (k) and turbulent dissipation rate (ε), the second order upwind method has been used.

These configurations are chosen because they have been validated against experimental results together with mesh independence studies [5,18]. The array configuration is validated computationally [35] and against the experiments of [36].

The rotor uses a Wortmann FX63-137 aerofoil and the comparison of CP (power) for both models shows that the BEM-CFD method predicts a slightly higher CP value of 0.44 compared to

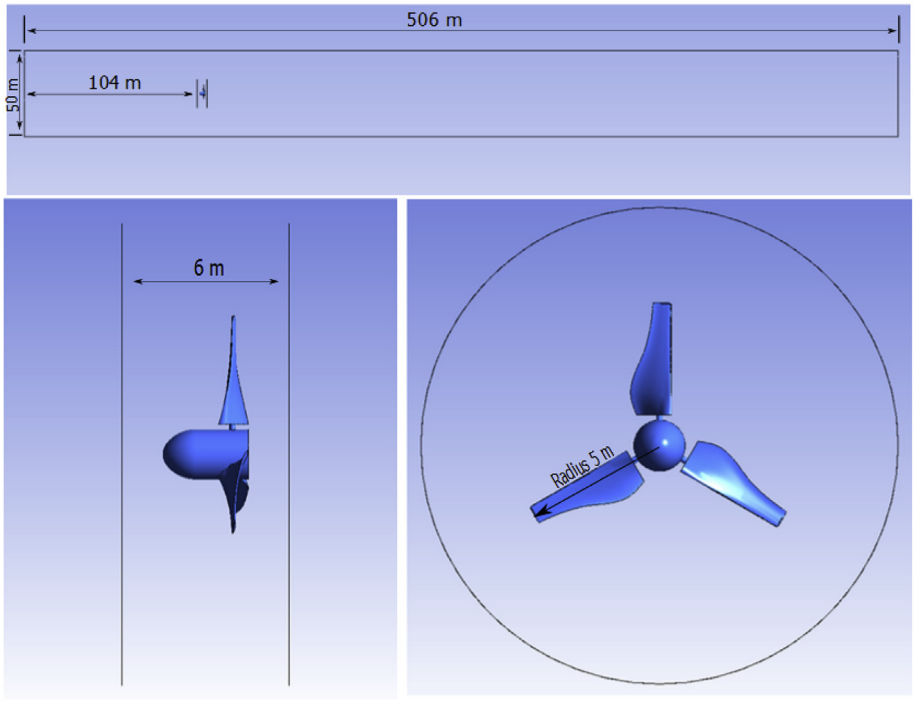

Fig. 2. The Blade Resolved Geometry (BRG) model domain.

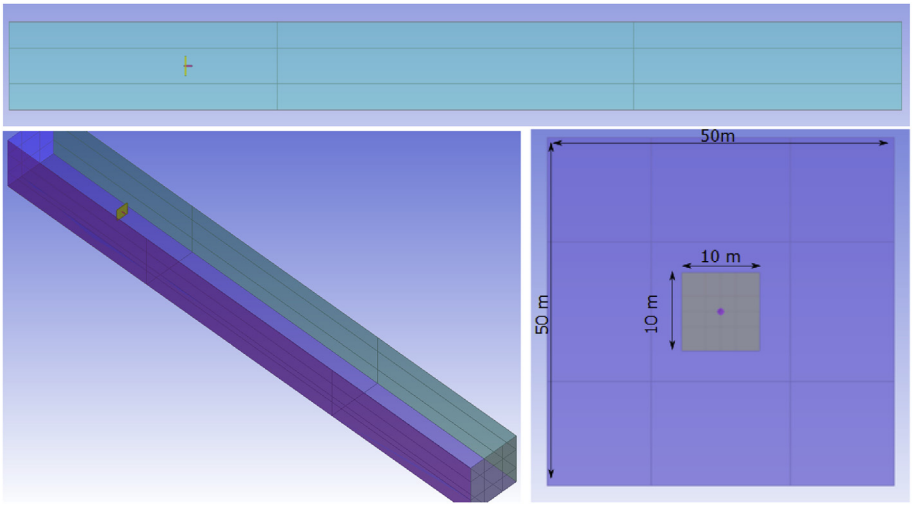

Fig. 3. The BEM-CFD single rotor model domain.

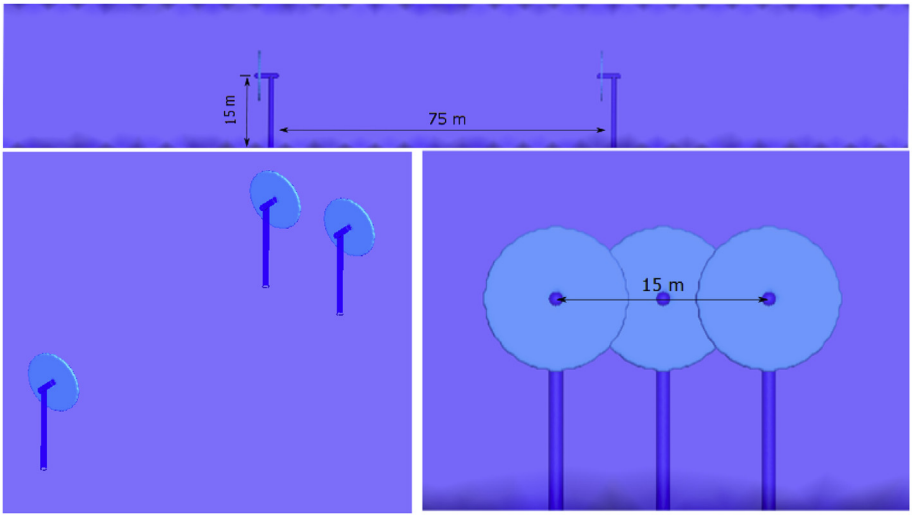

Fig. 4. The domain and BEM-CFD model for the Triangular Tidal Array.

0.40 for the BRG-CFD, and the CFa (axial force) for the BEM-CFD and BRG-CFD is 0.81 and 0.83, respectively [37]. The BRG-CFD results are published in Ref. [34] and also have good agreement with experimental results performed on a scale version of this rotor [34].

The diameter of this design is very close to the size of a prototype which is deployed in west Wales [38]. It is expected that larger rotors are more difficult to avoid, because they take up more of the vertical water column. However, larger rotors will rotate more slowly so should present less risk. In any case, all diameters of turbine run at similar tip speed ratios and the results here are reasonably transferable to other designs. With a lack of field data from different size devices, it is difficult to draw conclusions about these risk factors.

3.2. Fish swimming paths

To simulate the TST passage, it was considered that the fish swims along arbitrary streamtraces in the domain. A streamtrace is the trace of a massless particle from an initial location, and is tangential to the velocity field at every point along its length [39]. Streamtraces show the direction fluid flow within the flow domain. These streamtraces are chosen to simulate the most risk prone paths for the fish to swim through. The high risk and low risk location along the swimming path relative to the turbine were identified based on the maximum and minimum values of the pressure gradient.

In the tidal array configuration different scenarios could be defined (Fig. 15). First, fish can swim through the first turbine and then traverse the turbine in the second row. This is the most critical situation because the fish encounter two sudden pressure spikes in a matter of few seconds. A second scenario is; after passing through the first row of turbines, the fish do not traverse the second turbine. The third case considers that; it is also possible that the fish swim through the region 'between' the swept area of the two front turbines and then traverse a turbine in the second row. The third case is similar to the second case as the fish experience only one pressure spike.

4. Results

4.1. The pressure spike

After conducting the simulations for all cases, the pressure distributions are investigated. Due to the blocking effect of the TSTs,

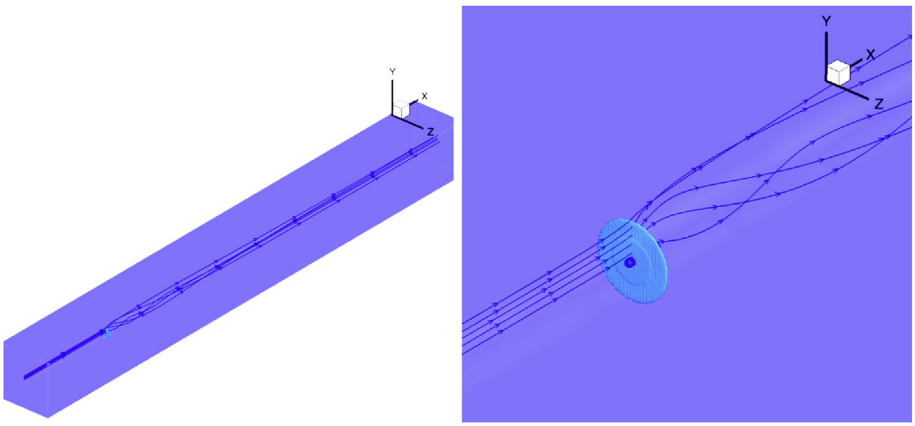

Fig. 5. Isometric representation of the streamtraces used in pressure graphs, single turbine and BEM-CFD method. The rotor diameter is 5 m, see Fig. 3 for domain extents.

there is an accumulation of pressure in front of the turbines. There is a large pressure change across the turbines, which is then followed by a gradual pressure recovery downstream.

For incompressible CFD fluid simulations, only dynamic pressure is calculated; static is assumed zero. However when assessing the risk to fish traversing vertically, then the dynamic pressure results from the CFD simulation need to be summed with the static pressure to provide the total pressure experienced by the fish. The static pressure is the density of the fluid(s) multiplied by acceleration due to gravity and the height of the fluid above the location of interest. In the case of the ocean, this is both the water column (hydrostatic pressure) and the air column above (atmospheric pressure).

In Sections 4.2 and 4.3, pressure is generally discussed in terms of dynamic quantities. The exception to this is when discussing the vertical movement of fish in the water column; in this case the quantities discussed are in terms of total pressure.

As mentioned in Section 3.1, all of the simulations are conducted using the peak flow with fixed pitch rotors. Based on this consideration the results presented here represent the highest pressure gradient that could occur, thus with lower flow speeds the pressure gradients are expected to be lower.

4.2. Single turbine

For the single turbine BEM-CFD model an examination of the streamtraces passing along the vertical symmetry line of the turbine is conducted (Fig. 5). The pressure values along each streamtrace are extracted as shown in Fig. 6. Streamtraces along the horizontal radius were also analysed but these were found to produce effects of smaller magnitude, so they are not reported here. Pressure is plotted against time to provide consistent data presentation with experiments [11]. This treatment affords easier comparison of the passage through a TST and a conventional hydroelectric turbine (Fig. 1). Pressure contours on a vertical slice through the rotor are shown in Fig. 7.

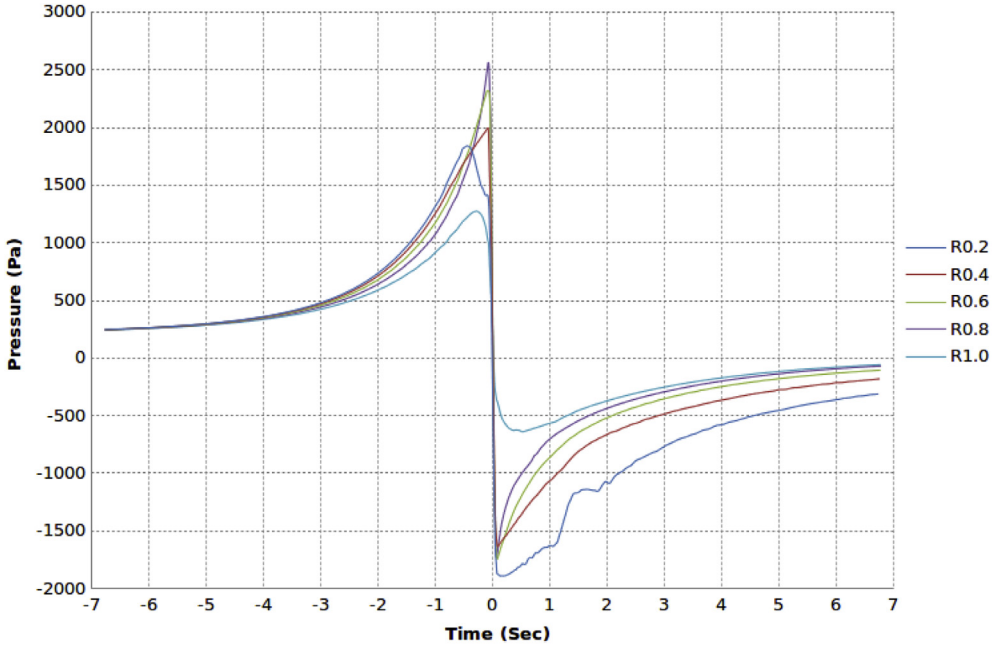

Fig. 6. Dynamic pressure change along the vertical section perpendicular to the hub of a tidal turbine passing the turbine from r = 1 m to r = 5 m for every meter from the centre of the turbine (BEM-CFD). The turbine outer radius R is 5 m and the radial locations shown are r = 0.2 (R = 1 m) to r = 1 (R = 5 m).

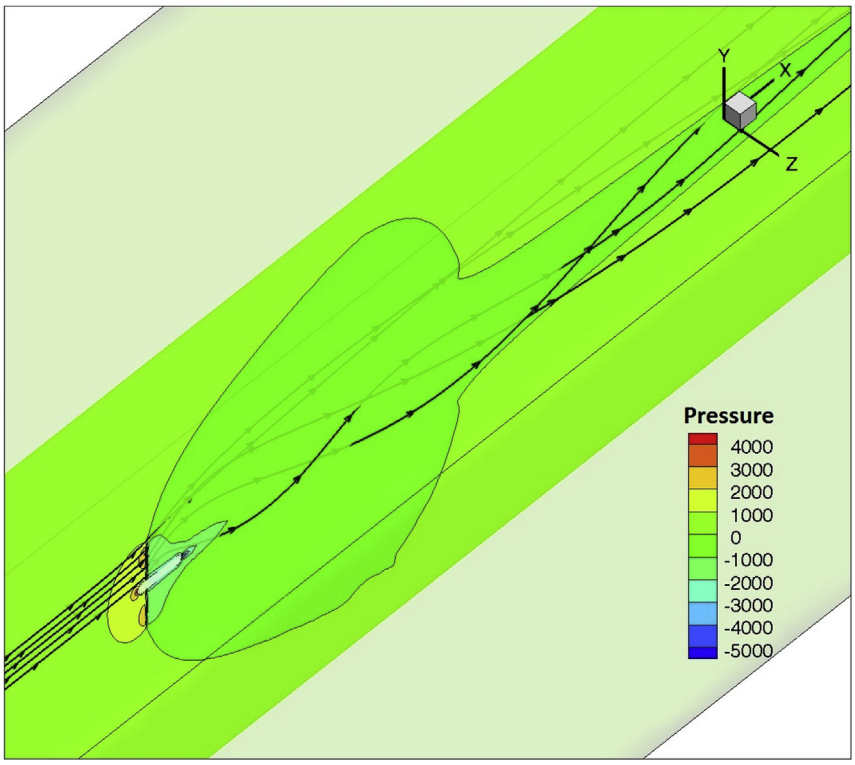

Fig. 7. Dynamic pressure contour at the vicinity of turbine along with the stream traces in a single array configuration tidal turbine (Pa). The rotor diameter is 5 m, see Fig. 3 for domain extents.

Fig. 6 shows that the pressure increases immediately in front of the turbine to the maximum value of nearly 2600Pa. This is followed by a decrease in pressure behind the turbine to a minimum value that is slightly lower than −1750Pa. Fig. 6 also shows that, as expected, the pressure recovers as the fish travel further away from the hydrofoils.

For the streamtrace near the hub of the turbine, the pressure recovery rate is slower than the other streamtraces (Fig. 6) and it

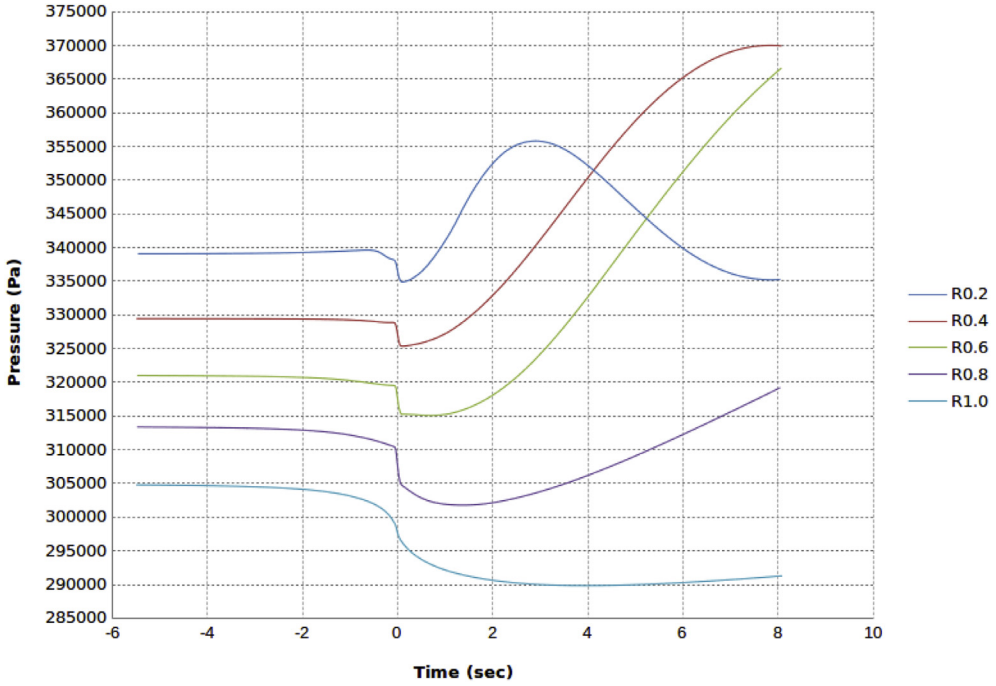

Fig. 8. Absolute pressure change along the vertical section perpendicular to the hub of a tidal turbine passing the turbine from r = 1 m to r = 5 m for every meter from the centre of the turbine including the effect of depth induced pressure (BEM-CFD). The turbine outer radius R is 5 m and the radial locations shown are r = 0.2 (R = 1 m) to r = 1 (R = 5 m).

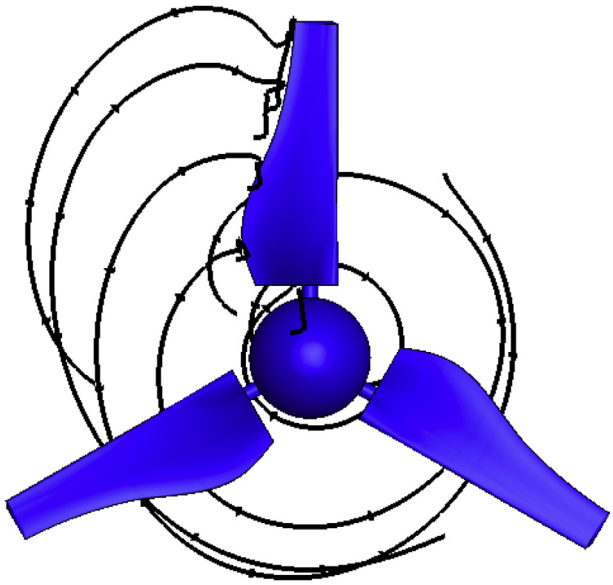

Fig. 9. Looking downstream towards the rotor, five streamlines are initiated close to the trailing edge of the hydrofoil. The streamlines show the subsequent downstream swirl pattern.

has another drop in the recovery phase. This occurs because this particular track passes behind the nacelle which has its own wake and eddies (Fig. 7). The pressure increase seen in front of the TST (Fig. 7) is the result of the resistance (or drag) of the device against the free stream flow. At the centre of this region is a further increase in pressure in front of the nacelle. The blockage affect of the nacelle effects the fish swimming along the streamtrace at 0.2R. Fish swimming at 0.2R would be exposed to a pressure spike for a longer period in comparison to fish swimming further from the nacelle.

Fig. 8 shows the total pressure change imposed on fish by both the TST passage (dynamic) and the hydrostatic pressure at the device location (static). It shows that for the radial distance of 3 m from the hub (0.6R), the fish experience an increase of about 50000Pa in nearly 8 s which is roughly equivalent to vertical travel of more than 5 m. This is equal to a 37.5 m/min vertical movement. For many fish this would not be normal behaviour [40]. However, in this study it is considered that the fish is acting like an object with no sense and power to swim away from the wake behind the turbine, whereas in real world conditions the fish have the ability to do that after the fish overcomes the initial disorientation of the pressure drop. Based on this assumption, the effect of the pressure change has been restricted to 8 s after passage through the turbine, during which period forced vertical migration is induced.

The same investigation has been considered for the BRG model. For this case it is obvious that the most critical areas are near the blades (i.e. the leading edge and trailing edge). Investigation of what happens close to the leading edge is out of the scope of this research. This is firstly because any fish that swims that close to the blade is in danger of being hit by the blade during the turbine passage [41], and secondly this study does not include shrouded TSTs (see Section 1). Assuming that one of the blades is in the vertical position the streamtraces are shown in Fig. 9. Corresponding pressure traces are shown in Fig. 10.

The BRG model also shows a pressure increase in front of the turbine followed by a sharp pressure decrease immediately behind the turbine (Fig. 10). However, the absolute maximum and minimum values for pressure in the BRG model are larger in comparison to the BEM-CFD model. In the BRG model the largest pressure drop of nearly 30,000 Pa happens close to the tip of the blade. For the other streamtraces in the radial direction the values are comparable to the range of the pressure changes for the BEM-CFD method.

Because of the nature of the BEM-CFD model, the dominant

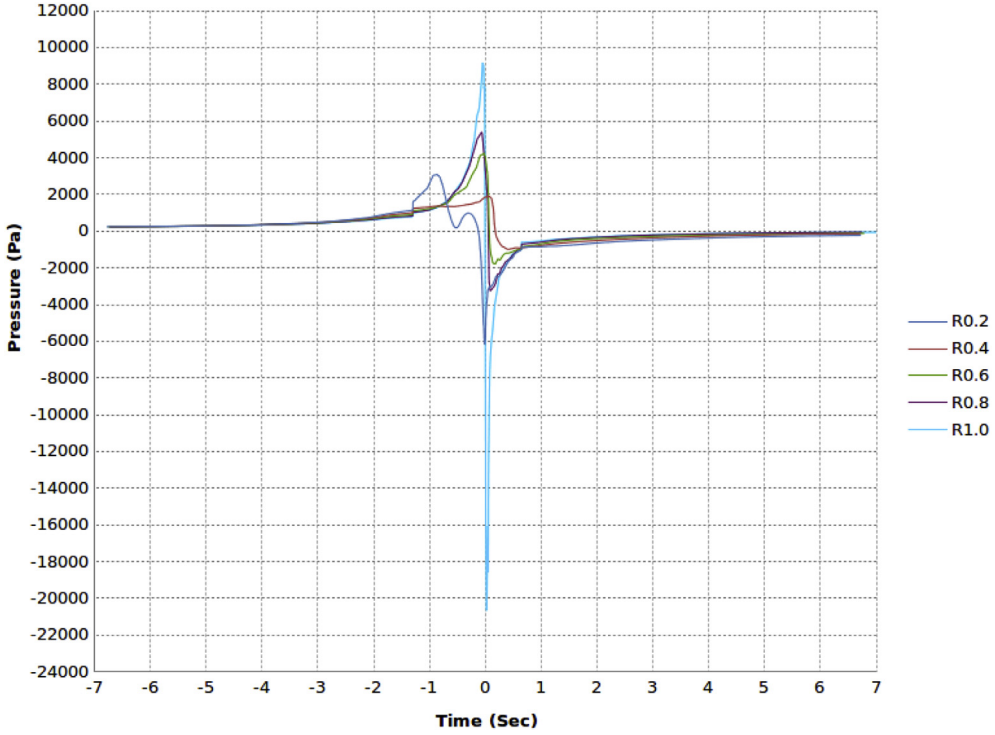

Fig. 10. Dynamic pressure change along the vertical section perpendicular to the hub of a tidal turbine passing the turbine from r = 1 m (0.2R) to r = 5 m (1.0R) for every meter from the centre of the turbine (BRG). The turbine outer radius R is 5 m and the radial locations shown are r = 0.2 (R = 1 m) to r = 1 (R = 5 m).

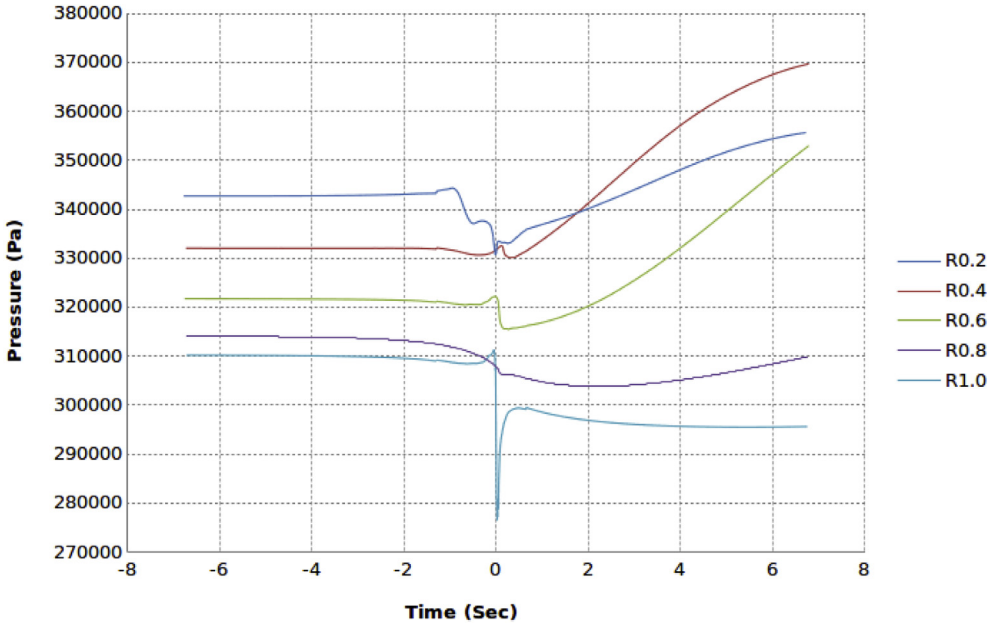

Fig. 11. Absolute pressure change along the vertical section perpendicular to the hub of a tidal turbine passing the turbine from r = 1 m to r = 5 m for every meter from the centre of the turbine including the effect of depth induced pressure (BRG).

effect of the hydrofoil is averaged over the circumferential region. This is in contrast to the BRG model where the further away from the trailing edge of the hydrofoil in the circumferential direction, the severity of the pressure change decreases. The BRG results show that it has a comparable pressure value to that of BEM-CFD at the location exactly in between two hydrofoils. As the leading edge of the next blade is approached, the pressure increases again.

The pressure change due to the vertical movement of the fish in the wake of the turbine (with the same assumption of the ability of the fish to swim out of the wake after 24 m) is shown in Fig. 11. The survival chance of the fish for all of the scenarios will be discussed at the end of this Section 4.4.

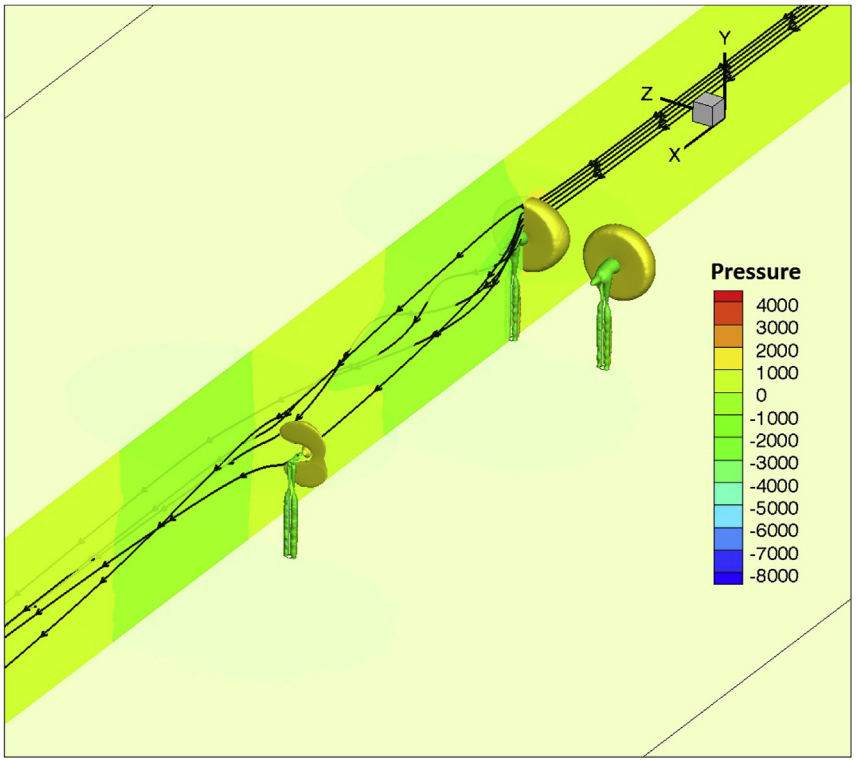

Fig. 12. Dynamic pressure isosurface at the vicinity of turbine along with the streamtraces passing along the vertical symmetry line of the first row turbine for a triangular array configuration tidal turbine (BEM-CFD). The rotor diameters are 5 m, see Fig. 4 for layout and domain extents.

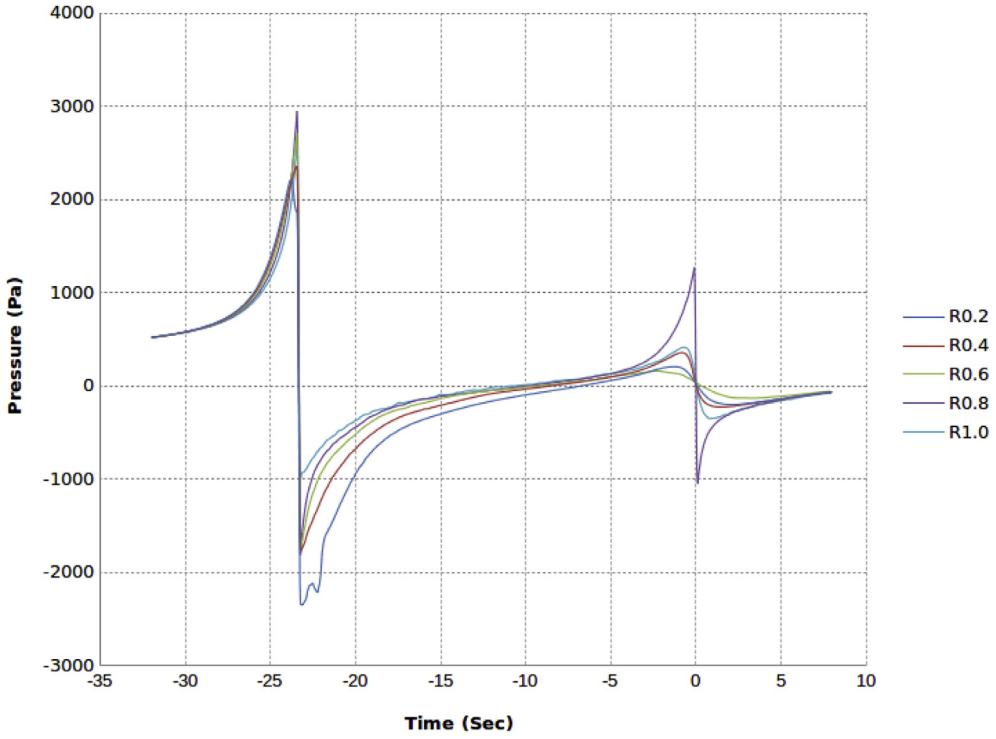

Fig. 13. Dynamic pressure change along the with the streamtraces passing along the vertical symmetry line of the first and second row turbines for a triangular array configuration tidal turbine from r = 1 m to r = 5 m for every meter from the centre of the Turbine (BEM-CFD).

4.3. Triangular Tidal Array

A triangular arrangement array has been simulated using the BEM-CFD approach. As described earlier, there are several assumptions that could be made here but the most critical one is the case of fish drifting into the second row turbine after passing through the first row turbines. To investigate this, paths of the streamtraces that are aligned vertically above the hub are plotted in

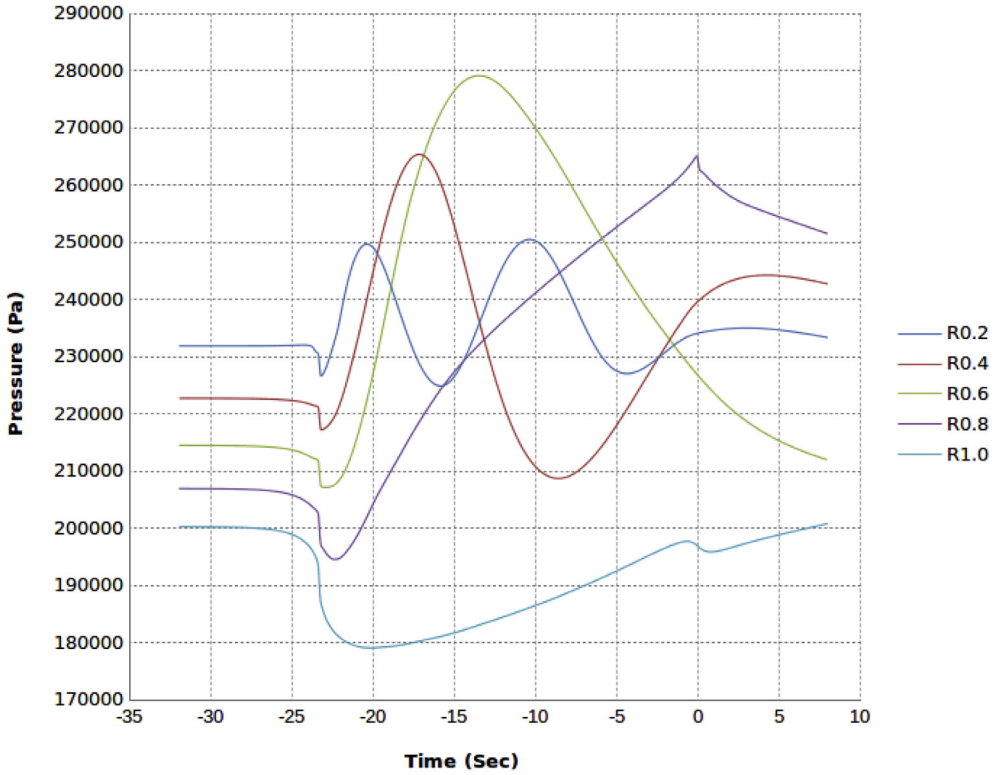

Fig. 14. Absolute pressure change, including the effect of depth streamtraces, along the streamtraces passing along the vertical symmetry line of the first and second row turbines for a triangular array configuration tidal turbine from r = 1 m to r = 5 m for every meter from the centre of the turbine (BEM-CFD).

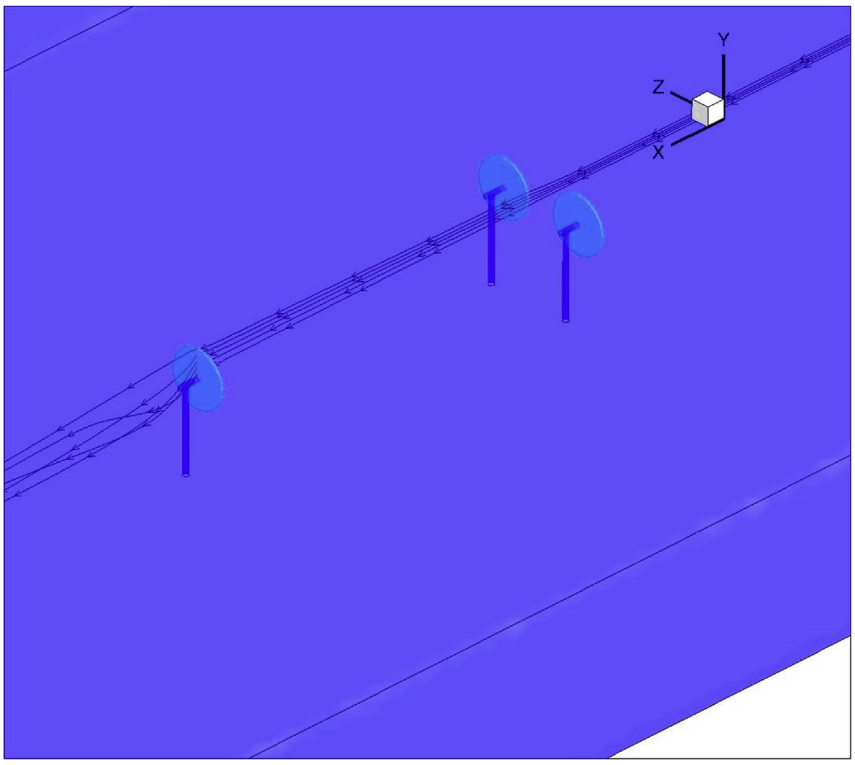

Fig. 15. The streamtraces passing along the vertical symmetry line of the second row turbine for a triangular array configuration tidal turbine (BEM-CFD). The rotor diameters are 5 m, see Fig. 4 for layout and domain extents.

Fig. 12. These results show that only the two streamtraces which are close to the tip of the first turbine (0.8R and 1.0R) go through the second turbine. While the range of pressure changes for the first row turbine is very close to the single array turbine (compare Figs. 6 and 13), the turbine in the second row has a lower pressure range because it is located in the shadow of the first row of turbines, and thus in a relatively low pressure region. For the streamtraces passing at 0.8R the pressure spike is significantly higher at the

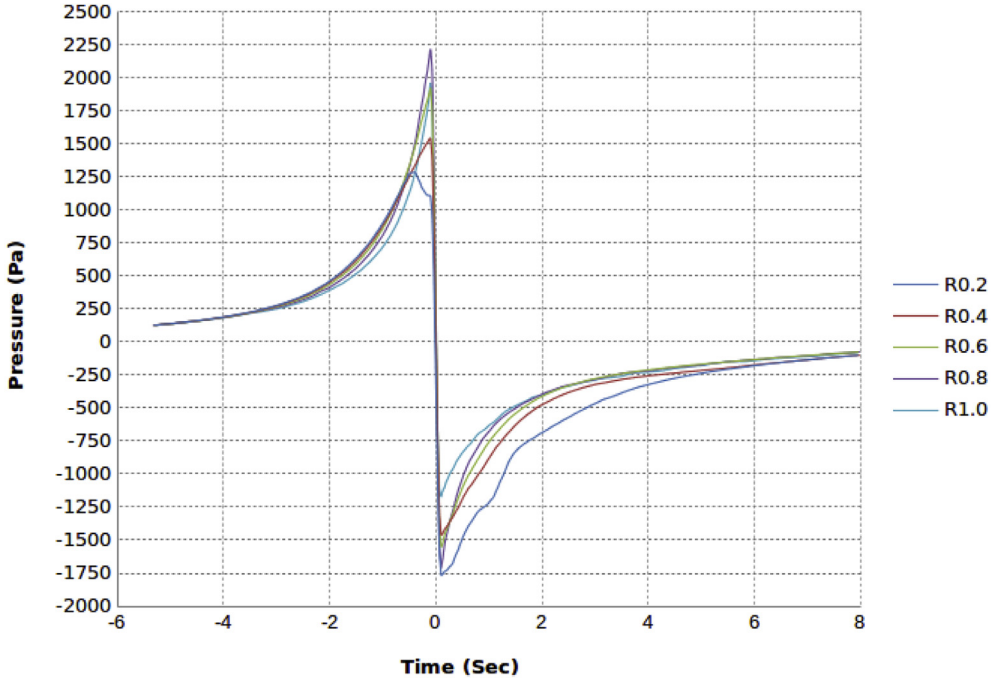

Fig. 16. Dynamic pressure change along the streamtraces passing along the vertical symmetry line of the second row turbine for a triangular array configuration tidal turbine from r = 1 m to r = 5 m for every meter from the centre of the turbine (BEM-CFD).

Table 3
Pressure change at the blade for the most critical streamtraces.

Position of the streamtraces	Maximum dynamic pressure before the turbine (Pa)	Minimum dynamic pressure after the turbine (Pa)	Pressure change or pressure drop (Pa)
Single Turbine at 0.8R (BEM-CFD)	2567	−1724	4291
Single Turbine at 1.0R (BRG)	9170	−20592	29,762

Table 4
Minimum pressure (P1), maximum pressure (P2) and swim bladder volume change for the most critical streamtraces in the wake of the turbine for a single device and triangular configuration tidal array.

Position of the streamtraces	P1 + Atm (Pa)	P2 + Atm (Pa)	Volume change percentage
Single Turbine at 0.6R with Depth Added Pressure (BEM-CFD) [Fig. 5, third stream trace from centre, Fig. 14, green line]	313,810	365,373	14% Decrease
Single Turbine at 0.6R with Depth Added Pressure (BRG) [Fig. 9, third stream trace from tip, Fig. 10, green line]	314,159	354,581	12% Decrease
Wake of Tidal Array, First Row Turbine with Depth Added Pressure at 0.6R (BEM-CFD) [Fig. 12, third stream trace from centre, does not pass through rear turbine, Fig. 14 green line]	205,911	277,841	26% Decrease

second turbine in comparison to the other streamtraces (Fig. 13). The reason is that this particular swim track is located closer to the hub of the second turbine in comparison to the other ones. The effect of water depth on pressure change is also investigated for this case, i.e. total pressure (Fig. 14). The same forced vertical migration that was observed at the single device, happens here.

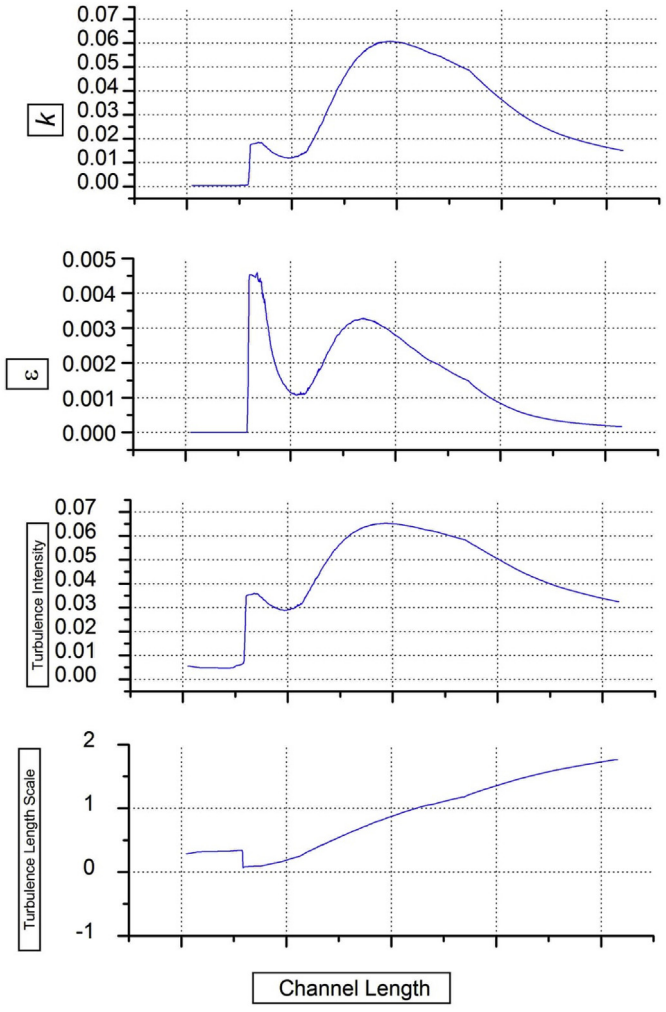

Fig. 17. Comparison of k, ε, turbulence length scale and turbulence intensity along the length of the channel (BEM-CFD).

In the second case investigated the fish swim in the space between the two turbines but then pass through the swept area of the second row turbine, as shown in Fig. 15. The streamtraces pass through the vertical symmetry line of the second row turbine. The pressure behaviour in the vicinity of the second row turbine is plotted in Fig. 16. This exhibits similar characteristics to pressure in the vicinity of a single turbine (Fig. 6), although the pressure range is smaller.

4.4. The swim bladder and Boyles Law

The literature review in Section 2.1 mentioned that the fish swim bladder obeys Boyles Law. The severity of the swim bladder volume change is an important factor in the survival chance of the fish (assuming the fish contains a swim bladders). With the premise that the water temperature is constant, it is reasonable to suppose that any pressure change on the surface of the fish maps directly to a change in volume of the swim bladder. As the modelling results show the pressure before and after the passage, it is possible to calculate the volume change of the swim bladder.

The following tables show the percentage change in swim bladder volume for the fish exposed to the most extreme conditions observed in the CFD results. Table 3 shows the dynamic pressure at the hydrofoil and the effect of depth related pressure on fish swimming in the wake behind the turbine is shown in Table 4. To aid in a direct comparison with [11], total pressure is used in Table 4, i.e. the sum of dynamic and static pressure.

4.5. Turbulence

Turbulence is a less significant issue in comparison to the pressure change during the turbine passage. It was mentioned in the literature review that there are two turbulence parameters that affect the survival rate: the turbulence length scale, which can cause disorientation or dizziness depending on the size of the fish, and the shear stress, which can cause torsion and deformation.

For the $k-\varepsilon$ turbulence model, the turbulence length scale is the ratio of turbulent kinetic energy to the energy dissipation rate. Further downstream of the turbine this value gets bigger because the rate of dissipation, ε, is greater than the kinetic energy k. This means that towards the end of the channel there are larger eddies in comparison to the upstream locations in the channel, however the intensity and energy of these vortices are actually decreasing. Therefore, large turbulence length scales are observed in a

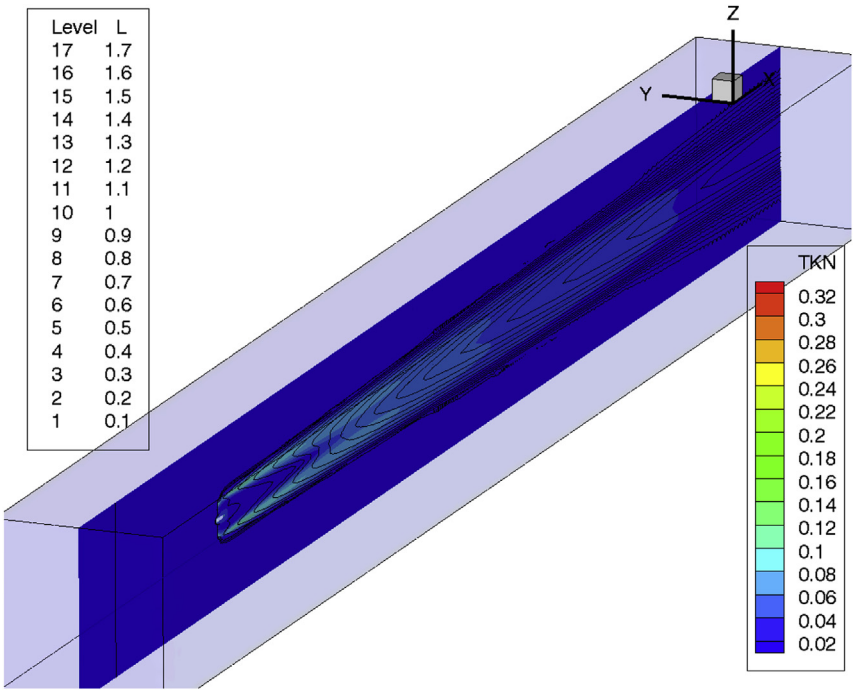

Fig. 18. Colour map of turbulence kinetic energy overlaid with the contours of turbulence length scale for a single turbine (BEM-CFD). The rotor diameter is 5 m, see Fig. 3 for domain extents.

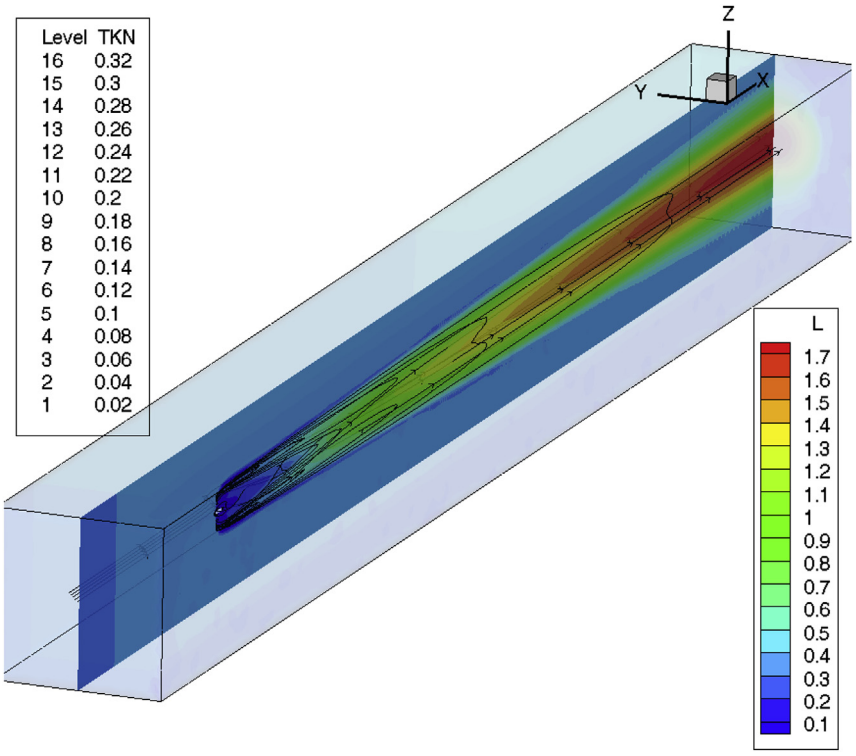

Fig. 19. Colour map of turbulence length scale overlaid with contours of turbulence kinetic energy for a single turbine (BEM-CFD). The rotor diameter is 5 m, see Fig. 3 for domain extents.

relatively low energy region (Fig. 17). This means that for the single device configuration, there might be a 1.7 m lengthscale eddy towards the end of the channel but it may not have the intensity to confuse the fish which could swim away (Fig. 18, Fig. 19). Disorientation is a critical issue for fish passing through a conventional hydroelectric turbine because it may cause the fish to hit the runner and walls of the draft tube. However this space restriction is not an issue in TSTs.

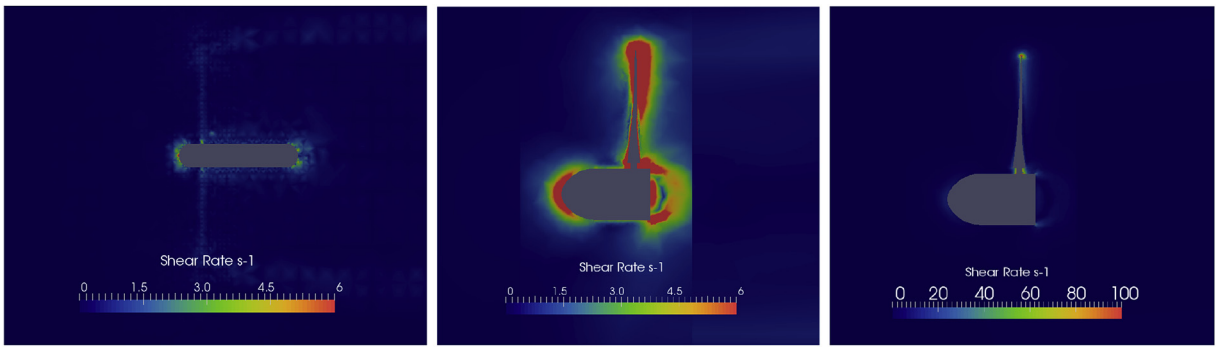

Fig. 20. The visualisations in this figure plot shear rate in/s. For the BEM-CFD model (left visualisation) the results are clipped to a maximum of 6/s thus highlighting the area of highest shear rate. The BRG-CFD model (centre) is visualised with the same range as BEM-CFD for comparison. The right panel shows the same data as the centre, but set to a maximum of 100/s to highlight the region of high shear rate.

The amount of shear rate was also investigated, see Fig. 20. The results show that for the BEM-CFD model, the maximum value is 12.7/s for the single turbine and for the tidal array configuration the maximum value is 12.5/s. For the BRG model the peak value is slightly over 300/s but this amount of shear rate occurs only in very small locations near the blade tip ($x = 0$ m, $r = 5$ m).

5. Discussion

TSTs differ from conventional hydroelectric turbines with respect to pressure change across the device, and turbulent shear rates through and downstream of the device. The CFD results indicate how the pressure changes and shear rates across a TST are noticeably less than what is generally found within conventional hydroelectric turbines.

Two significant phenomena are investigated that could have an effect on the survival of fish that pass between the blades of a turbine, namely, 'rapid and excessive pressure change' and 'high shear and turbulence levels'. A review of previous studies on the interaction of fish and conventional hydroelectric turbines showed that the main issue is the head difference before and after the turbine; this is not the case for TSTs.

The authors of [32] studied fish mortality and injury by introducing them to a high shear environment in the laboratory. The fish were exposed to a submerged jet with exit velocities ranging from 0 up to 21.3 m/s. It was observed that fish injury and mortality became significant where shear rates were greater than 495/s. The turbulence or velocity shear rates calculated from the computational models (discussed earlier) show much lower levels than that noted as critical by Ref. [32]. An exception to this is a small region close to the tip of the hydrofoil (within $\approx$0.01 m from the hydrofoil tip). However, these relatively small areas are unlikely to affect the mortality rate of the fish passing through a TST.

The main organ in fish affected by a rapid pressure change is their swim bladder (where applicable). Tests show that physostomous fish can tolerate a low-head turbine passage better in comparison to physoclistous fish with less visible external damage [30]. Apart from the type of the swim bladder, the acclimatisation of fish to a higher pressure prior to the passage might have some influence on the pressure-related mortality [14]. A notable observation is the exposure time to pressure changes. The pressure spike in conventional hydroelectric turbines occurs in a period of about 0.2 s [11] while for a TST it occurs in a time period of 0.5–1 s (Fig. 6).

Some of the results presented in this paper show uncontrolled vertical movement through the water column, mostly due to wake rotation downstream of the turbine (Figs. 5, 7, 12 and 15). However, fish may react to such changes and will likely attempt to swim against this effect. Alternatively the fish may swim with the flow, or even drift. These scenarios are more likely if the fish have been disoriented or are unable to control their swim bladder effectively [32], [14]. Therefore, the CFD results presented here may be conservative (in an engineering sense), actual results may be less severe having a lower 'rate of change of pressure' (pressure gradient) which in turn may have less effect on the fish population.

To adjust to their depth preference, fish need to regulate the gases in their swim bladder to achieve the desired effect. It is likely that the sudden changes in pressure whilst traversing a TST (as discussed above) will effect the fish to some degree i.e. either temporary effects such as being disorientated, or permanent damage [32], [14]. Thus there is a chance during and post traversal of a TST that the fish are not able to regulate their swim bladder. This scenario is likely to affect their ability to complete other basic biological functions, i.e. feeding, locomotion, and reproduction. During the period of time prior to recovery, the fish may also be predated. It must be noted that not all fish have swim bladders, and the size of the fish matters. This is an important consideration while drawing conclusions.

6. Conclusions

This paper presents a study of the environmental effects of TSTs, paying particular attention to pressure and turbulence fields. This work then discusses how these flow characteristics may affect fish with swim bladders. It appears that there is a greater chance of survival in comparison to passage through conventional hydroelectric turbines. However, it must be recognised this is limited to observations of fish with swim bladders and does not include strike potential. A new data interpretation approach is proposed; the rate of change of pressure with time along a streamtrace.

Providing that the fish do not experience a blade strike, this work indicates that, in most cases, pressure and turbulence are unlikely to cause immediate mortality based on relative comparison with changes observed at conventional hydroelectric turbines. This study provides important information for collision risk modelling and fills an information gap highlighted in the previous study by Ref. [7].

Any study related to the survival rate of fish during turbine passage is highly species specific so it is not possible to indicate that one particular design is 100% fish friendly. For any proposed TST installation site it will be necessary to carry out an environmental assessment of the location. Information related to the biology of the species in the proposed area can then be used to calculate survival rates related to the design of individual TSTs and also the design of TST arrays using the techniques presented in this paper.

In relation to turbulence, shear stress effects are likely to be observed very close to the blades and further work should be undertaken to understand 'near miss' scenarios.

Acknowledgements

The Authors wish to acknowledge the financial support of the Welsh Assembly Government, the Welsh European Funding Office, and the European Regional Development Fund Convergence Programme. The work was also supported by the EPSRC funded "Extension of UKCMER Core Research, Industry and International Engagement" project (EP/M014738/1). The Author(s) acknowledge(s) the financial support provided by the Welsh Government and Higher Education Funding Council for Wales through the Sêr Cymru National Research Network for Low Carbon, Energy and Environment. (C001822).

References

[1] A.B. Gill, Offshore renewable energy: ecological implications of generating electricity in the coastal zone, J. Appl. Ecol. 42 (4) (2005) 605–615.
[2] G.W. Boehlert, A.B. Gill, Environmental and ecological effects of ocean renewable energy development: a current synthesis, Oceanogr. Soc. 23 (2) (2010) 68–81.
[3] A.S. Bahaj, Marine current energy conversion: the dawn of a new era in electricity production, Philosophical Trans. R. Soc. A Math. Phys. Eng. Sci. 371 (1985) (2013), 20120500.
[4] J. McNaughton, S. Rolfo, D. Apsley, T. Stallard, P. Stansby, CFD power and load prediction on a 1MW tidal stream turbine with typical velocity profiles from the EMEC test site, in: Proceedings of the 10th European Wave and Tidal Energy Conference, 2013, pp. 1–4, 2nd–5th September, Aalborg.
[5] M. Edmunds, R. Malki, A. Williams, I. Masters, T. Croft, Aspects of tidal stream turbine modelling in the natural environment using a coupled bemcfd model, Int. J. Mar. Energy 7 (0) (2014) 20–42.
[6] P. Romero-Gomez, M.C. Richmond, Simulating blade-strike on fish passing through marine hydrokinetic turbines, Renew. Energy 71 (2014) 401–413.
[7] L. Hammar, L. Eggertsen, S. Andersson, J. Ehnberg, R. Arvidsson, M. Gullström, S. Molander, A probabilistic model for hydrokinetic turbine collision risks: exploring impacts on fish, PloS one 10 (3) (2015) e0117756.
[8] H.A. Viehman, G.B. Zydlewski, Fish interactions with a commercial-scale tidal energy device in the natural environment, Estuaries Coasts 38 (1) (2015) 241–252.
[9] C. Tomichek, J. Colby, M. Bevelhimer, M.A. Adonizio, 0, Parameter Updates to Probabilistic Tidal Turbine Fish Interaction Model, vol. 0, National Hydropower Association, 2016, 0-0.
[10] R. Malki, I. Masters, A.J. Williams, T.N. Croft, in: The Variation in Wake Structure of a Tidal Stream Turbine with Flow Velocity, in: MARINE 2011, IV International Conference on Computational Methods in Marine Engineering, Springer, 2011, pp. 137–148.
[11] J.M. Becker, C.S. Abernethy, D.D. Dauble, Identifying the effects on fish of changes in water pressure during turbine passage, Hydro Rev. 22 (5) (2003) 32–42.
[12] G. Čada, J. Loar, L. Garrison, R. Fisher Jr., D. Neitzel, Efforts to reduce mortality to hydroelectric turbine-passed fish: locating and quantifying damaging shear stresses, Environ. Manag. 37 (6) (2006) 898–906.
[13] H.C. Buckland, I. Masters, J.A. Orme, T. Baker, Cavitation inception and simulation in blade element momentum theory for modelling tidal stream turbines, in: Proceedings of the Institution of Mechanical Engineers, Part a: Journal of Power and Energy, vol. 227, 2013, pp. 479–485, 4.
[14] S. Amaral, G. Hecker, N. Pioppi, Fish Passage through Turbines: Application of Conventional Hydropower Data to Hydrokinetic Technologies, Tech. Rep, EPRI (Electric Power Research Institute), 2011. Tech. Rep. 1024638.
[15] E. Zangiabadi, Using 3d-cfd Methods to Investigate Hydrology of Oceans and Fish Passage through Tidal Stream Turbines, Ph.D. Thesis, Engineering, Swansea University, 2015.
[16] C.C. Coutant, R.R. Whitney, Fish behavior in relation to passage through hydropower turbines: a review, Trans. Am. Fish. Soc. 129 (2) (2000) 351–380.
[17] M. Dadswell, R.A. Rulifson, Macrotidal estuaries: a region of collision between migratory marine animals and tidal power development, Biol. J. Linn. Soc. 51 (1–2) (1994) 93–113.
[18] M. Edmunds, A.J. Williams, I. Masters, T.N. Croft, An enhanced disk averaged cfd model for the simulation of horizontal axis tidal turbines, Renew. Energy 101 (2017) 67–81. http://dx.doi.org/10.1016/j.renene.2016.08.007. http://www.sciencedirect.com/science/article/pii/S096014811630708X.
[19] A. Mason-Jones, Performance Assessment of a Horizontal Axis Tidal Turbine in a High Velocity Shear Environment, Ph.D. Thesis, Cardiff University, 2010.
[20] J.K. Horne, K. Sawada, K. Abe, R.B. Kreisberg, D.H. Barbee, K. Sadayasu, Swimbladders under pressure: anatomical and acoustic responses by walleye pollock, ICES J. Mar. Sci. J. du Conseil (2009) fsp101.
[21] D. A. Neitzel, M. C. Richmond, D. D. Dauble, R. P. Mueller, R. A. Moursund, C. S. Abernethy, G. R. Guensch, G. Cada, reportLaboratory Studies on the Effects of Shear on Fish, Report to the US Dept. of Energy Idaho Operations Office, Idaho Falls, ID.
[22] S.V. Amaral, M.S. Bevelhimer, G.F. Čada, D.J. Giza, P.T. Jacobson, B.J. McMahon, B.M. Pracheil, Evaluation of behavior and survival of fish exposed to an axial-flow hydrokinetic turbine, North Am. J. Fish. Manag. 35 (1) (2015) 97–113.
[23] M. Watson, Allowable Gas Supersaturation for Fish Passing Hydroelectric Dams. Task 8. Bubble Reabsorption in a Simulated Smolt Bypass System-Concept Assessment, 1995.
[24] I.N. Levine, Physical Chemistry, McGraw-Hill Inc, 1995.
[25] P. Tytler, J. Blaxter, The effect of swimbladder deflation on pressure sensitivity in the saithe pollachius virens, J. Mar. Biol. Assoc. U. K. 57 (04) (1977) 1057–1064.
[26] G. Čada, in: Shaken, Not Stirred: the Recipe for a Fish-friendly Turbine, in: Waterpower, vol. 1, American Society Civil Engineers, 1997, pp. 374–382.
[27] S.L. Traxler, B.R. Murphy, T.L. Linton, Subsediment seismic explosions do not injure caged fishes in a freshwater reservoir, J. Freshw. Ecol. 8 (1) (1993) 73–75.
[28] F. Sotiropoulos, A Numerical Model for Calculating Fish Passage through Hydraulic Powerplants, 1999.
[29] G.F. Čada, C.C. Coutant, R.R. Whitney, Development of Biological Criteria for the Design of Advanced Hydropower Turbines Tech. Rep., E. S. Division and O. R. N. Laboratory, Oak Ridge, 1997.
[30] A.W. Turnpenny, G. Struthers, K.P. Hanson, A Uk Guide to Intake Fish-screening Regulations, Policy and Best Practice, Energy Technology Support Unit, Harwell, 1998. www.thaaquatic.co.uk/publications.htm.
[31] USACE, Turbine Fish Passage Survival Workshop, Tech. Rep., U.S, Army Corps of Engineers, Portland, 1995.
[32] D.A. Neitzel, D.D. Dauble, G. Čada, M.C. Richmond, G.R. Guensch, R.P. Mueller, C.S. Abernethy, B. Amidan, Survival estimates for juvenile fish subjected to a laboratory-generated shear environment, Trans. Am. Fish. Soc. 133 (2) (2004) 447–454.
[33] T. Cook, G. Hecker, S. Amaral, P. Stacy, F. Lin, E. Taft, reportFinal Report pilot Scale Tests Alden/concepts Nrec Turbine, Alden Research Lab., Holden, MA.
[34] A. Mason-Jones, D.M. O'Doherty, C.E. Morris, T. O'Doherty, C. Byrne, P.W. Prickett, R.I. Grosvenor, I. Owen, S. Tedds, R. Poole, Non-dimensional scaling of tidal stream turbines, Energy 44 (1) (2012) 820–829.
[35] R. Malki, I. Masters, A.J. Williams, T. Nick Croft, Planning tidal stream turbine array layouts using a coupled blade element momentum–computational fluid dynamics model, Renew. Energy 63 (2014) 46–54.
[36] L. Myers, A. Bahaj, An experimental investigation simulating flow effects in first generation marine current energy converter arrays, Renew. Energy 37 (1) (2012) 28–36.
[37] I. Masters, A.J. Williams, T.N. Croft, M. Togneri, M. Edmunds, E. Zangiabadi, I. Fairley, H. Karunarathna, A comparison of numerical modelling techniques for tidal stream turbine analysis, Energies 8 (8) (2015) 7833–7853.
[38] TEL, DeltaStream Demonstrator Project Ramsey Sound, Pembrokeshire, 2009. http://www.marineenergypembrokeshire.co.uk/wp-content/uploads/2012/10/TEL-ES-NT.pdf. Retrieved: May 2015.
[39] M. Edmunds, R.S. Laramee, G. Chen, N. Max, E. Zhang, C. Ware, Surface-based flow visualization, Comput. Graph. 36 (8) (2012) 974–990. http://dx.doi.org/10.1016/j.cag.2012.07.006. http://www.sciencedirect.com/science/article/pii/S0097849312001355.
[40] A. Redden, M. Stokesbury, Acoustic Tracking of Fish Movements in the Minas Passage and Force Demonstration Area: Pre-turbine Baseline Studies, 2011-2013.
[41] T. J. Carlson, J. Elster, M. Jones, B. Watson, A. Copping, M. Watkins, R. Jepsen, K. Metzinger, Assessment of Strike of Adult Killer Whales by an Openhydro Tidal Turbine Blade, Pacific Northwest National Laboratory technical report, PNNL-21177 (prepared for US Department of Energy).